© 3rd IAHR Europe Congress, Book of Proceedings, 2014, Porto - Portugal. ISBN 978-989-96479-2-3

LONGITUDINAL DEVELOPMENT OF COMPOUND CHANNEL FLOWS

JOÃO NUNO FERNANDES [1], JOÃO BENTO LEAL [2] & ANTÓNIO HELENO CARDOSO[3]

[1] *National Laboratory for Civil Engineering, Lisbon, Portugal*
jnfernandes@lnec.pt

[2] *UNIDEMI & Faculdade de Ciências e Tecnologia, Univ. Nova de Lisboa, Caparica, Portugal*
jleal@fct.unl.pt

[3] *Instituto Superior Técnico, Lisbon University, Lisbon, Portugal*
antonio.cardoso@ist.utl.pt

Abstract

The longitudinal development of compound channel flow and the corresponding mixing and boundary layers are investigated. An experimental campaign was carried out in a laboratory compound channel. Six uniform flows were generated comprising (i) three on floodplains made of polished concrete and (ii) three on synthetic grass covering the floodplains.

The shallowness and the floodplain roughness effects on the longitudinal development of the streamwise velocities and of the lateral shear stress are also evaluated.

Keywords: *mixing layer, compound channel, main channel, floodplain*

1. Introduction

Rivers frequently acquire a compound channel configuration during floods as the flow occupies the floodplains. In compound channels, important interactions occur between the faster flow in the main channel and the slower flow in the floodplains. This velocity difference and the associated gradient are responsible for interfacial large-scale vortices with vertical axis. The interactions between the two flows imply the exchange of mass and momentum among them, controlled by the mixing layer originated between the two flows.

To understand the development of the mixing layer, several studies have been developed over the last decades (*e.g.* Wygnanski and Fiedler 1970 or Yule 1972). Chu *et al.* (1983) pointed out the importance of knowing the transverse extent of the mixing layer as well as the stabilizing influence of the bottom friction. The width of the mixing layers is defined by the width of the coherent structures responsible for the lateral momentum transfer (Booij and Tukker 2001).

Depending on the water depth, two types of mixing layers can be distinguished: the plane mixing layer and the shallow-water mixing layer. The latter can be generated by (i) flows in straight channel with lateral roughness changes; (ii) confluences of flows with different velocities and (iii) compound channel flows (Vermaas *et al.* 2011).

In plane mixing layers, the velocity gradient between two streams is a source of turbulent kinetic energy. In the first part of the interaction, two-dimensional turbulent structures are generated.

Further downstream, these structures become unstable and disintegrate into three dimensional turbulence (Uijttewaal and Booij 2000). Alavian and Chu (1985) found the same similarity between compound channel flows and plane mixing layers but they pointed out the stabilizing effect of the bottom friction.

For the study of the shallowness effect on the development of mixing layers, Uijttewaal and Booij (2000) carried out two experiments in a single channel where two flows with different velocities interact. The bottom friction affected the streamwise development of the mixing layer due to (i) the decrease of the velocity gradient and to (ii) the suppression of the Kelvin-Helmholtz instabilities that govern the spreading of that layer. For the higher water depth, the mixing layer behaves as a plane mixing layer, and self-similarity is maintained. Analysing the power density spectra for the velocity fluctuations in spanwise direction for the two flows, Uijttewaal and Booij (2000) observed, for higher water depth, a clear peak with a slope of –3, revealing the large turbulence structures. The peak is more pronounced and moves to lower frequencies in the streamwise direction. For the lower water depth, the peak is detectable but it is much smaller and vanishes in the downstream cross sections.

According to the dominating flow characteristics, Booij and Tukker (2001) identified three regions in the longitudinal development of shallow-water mixing layers. In the first region, downstream the junction of the flows, the width of the layer is smaller than the water depth and the influence of the bottom on the mixing layer is small. In this region, the flow develops as a free mixing layer but the bottom turbulence can slightly increase the initial spreading rate. In the second region, the bottom friction has a major influence on the development of the mixing layer, leading to a decrease of its spreading rate. Here, horizontal large-scale eddies (called macro-vortices) develop with dimensions larger than the water depth. In the third region, these macro-vortices display horizontal dimensions much larger than the water depth. The stabilizing influence of the bottom friction suppresses the generation of new large-scale eddies, leading to the equilibrium of the mixing layer.

In this work, the flow development in the longitudinal direction of a compound channel and the corresponding mixing layer width will be analysed. After the verification of the boundary layer development in the centre of the main channel, for one flow case, the longitudinal evolution of the mixing layer width, of the streamwise velocity and of the lateral shear stress will be analysed. For this propose, velocity measurements in four cross sections are analysed for six uniform flows: (i) three on floodplains made of polished concrete and (ii) three on synthetic grass covering the floodplains.

2. Experimental setup and measuring equipment

Experiments were carried out in a 10.0 m long and 2.00 m wide symmetrical compound channel. Its cross section is presented in Figure 1 and consists of two equal rectangular floodplains (floodplain width B_{fp} = 0.7 m) and one trapezoidal main channel (bank full height, h_b = 0.1 m, main channel width, B_{mc} = 0.6 m, and 45° lateral bank slope, s_y = 1). In Figure 1, h_{mc} and h_{fp} are the main channel and the floodplain flow depths, respectively.

The channel bed is made of polished concrete and its longitudinal slope is s_0 = 0.0011. Three experiments were performed for the original polished concrete bottom (smooth boundary), while another three were run with synthetic grass on the floodplains (rough boundary). Preliminary tests for the characterization of the bed roughness indicated that Manning's coefficient is n = 0.0092 $m^{-1/3}s$ for the polished concrete and n = 0.0172 $m^{-1/3}s$ for the synthetic grass.

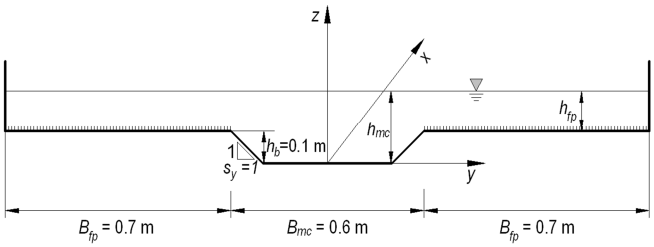

Figure 1. Schematic representation of the compound channel.

Separated inlets for the main channel and for the floodplains were installed by adopting the suggestion of Bousmar *et al.* (2005). For each inlet, the flow discharge was controlled with a valve and monitored through an electromagnetic flow meter with accuracy of ± 0.1 l/s. At the downstream end of the flume, independent tailgates for each sub-channel were used to adjust the water levels in the flume.

Water surface levels were surveyed with a point gauge (accuracy of ±0.3 mm) in 9 cross sections at 12 lateral positions per cross section.

Velocity measurements were carried out with a side looking Acoustic Doppler Velocimeter (ADV-vectrino). The acquisition time was fixed in 3 min at each measuring position, at a sampling frequency of 100 Hz. The velocity data were despiked with the filter of Goring and Nikora (2002). Only correlations and SNR higher than 70% and 15 dB, respectively, were considered. To align the ADV probe with the longitudinal direction, the pitch angle was slightly modified to get a depth averaged transverse velocity, V, equal to 0 near the floodplain sidewall. This correction was taken into account in the computation of the local mean velocity and the velocity fluctuations (*cf.* Roy *et al.* 1996). After verifying the symmetry of the flow conditions, only half of the cross section was investigated. In the half cross section, the measuring mesh comprised 22 measuring verticals, 3 measuring points per vertical in the floodplain (between $0.4h_{fp}$ and $0.8h_{fp}$) and 7 in the main channel (between $0.10h_{mc}$ and h_b+$0.8h_{fp}$).

The longitudinal development of the compound channel flow and the corresponding mixing and boundary layers was analysed. For this purpose, velocity measurements were also performed in cross sections 1.1 m, 3.0 m, 5.0 m and 7.5 m from the inlet section. Additional measurements were made in the centre of the main channel.

3. Control variables and parameters

For a given flow depth, the subsection discharge distribution corresponding to uniform flow was not known a priori. An iterative procedure was followed to impose it at x = 0 m (*cf.* Fernandes *et al.* 2012). The experimental conditions are listed in Table 1, where apart from the variables previously defined, Q_{mc} and Q_{fp} are the main channel and the floodplain discharges, respectively, and $h_r = h_{fp}/h_{mc}$ stands for the relative floodplain flow depth. The reference of each experiment, included in the first column of Table 1, is to be read as: "hr" followed by "percent relative depth" and by "s" or "r" (for smooth and rough floodplains, respectively). Froude numbers are presented per subsection, $Fr_i = U_i/(gR_i)^{1/2}$, where R is the hydraulic radius and subscript i stands for either main channel, *mc*, or floodplain, *fp*. The flow is subcritical for all tests, which is consistent with the use of three independent downstream gates to control the flow depth in each subsection. The Reynolds numbers, $Re = 4U_iR_i/\nu$ (ν being the kinematic viscosity) and the floodplain relative roughness, $k/(4R)$ (k being the absolute roughness), are also included in Table 1.

In view of the Reynolds number and the relative roughness of each subsection, it can be concluded that the flow is transition turbulent in the main channel and on the original polished concrete floodplains; it is rough turbulent when the floodplain is covered with synthetic grass.

Table 1. Experimental flow conditions.

Flow reference	Floodplain flow	h_{mc} (m)	h_r (-)	Q_{mc} (l.s^{-1})	Q_{fp} (l.s^{-1})	Fr_{mc}	Fr_{fp}	Re_{mc} (x10^5)	Re_{fp} (x10^5)	Floodplain relative roughness, $k/(4R)$
hr15s	Transition turbulent	0.1172	0.15	38.8	6	0.69	0.61	2.25	0.17	0.0022
hr20s	Transition turbulent	0.1220	0.19	42.2	11.2	0.70	0.78	2.45	0.31	0.0017
hr30s	Transition turbulent	0.1402	0.30	54.2	26.4	0.70	0.76	3.17	0.66	0.0009
hr15r	Rough turbulent	0.1192	0.15	35.1	3.7	0.61	0.32	2.04	0.10	0.0885
hr20r	Rough turbulent	0.1244	0.21	39.3	7.3	0.63	0.44	2.28	0.20	0.0697
hr30r	Rough turbulent	0.1450	0.31	42.3	16.6	0.52	0.41	2.45	0.44	0.0378

4. Flow development in the longitudinal direction

4.1 Boundary layer development

Near fixed walls, the flow velocity increases from zero at the wall to a value that, in the case of unbounded-layer flows, corresponds to external frictionless flow (Schlichting 1968). The area corresponding to that change in the velocity is the so-called boundary layer and the concept is due to Prandtl. In open-channel flows, the boundary layer of fully developed flows occupies the entire flow depth.

The evolution of the streamwise velocity along the longitudinal axis of the main channel was assessed for the flow case hr030s. For that purpose, vertical profiles of the streamwise velocity were measured in six cross sections. The results are presented in Figure 2, where the logarithmic-law profile, with parameter B = 5.1, is also plotted (dashed blue lines).

The streamwise velocity evolves longitudinally and becomes approximately self-similar between x = 7 m and x = 8 m where the universal log-law reasonably fits the measurements. At the most downstream cross section, there may be some influence of the downstream gates. Keeping in mind that a compound channel flow is being analysed, some influence of 3D turbulence is expected in the centre of the channel.

Therefore, other small discrepancies are ascribable to the interaction between main channel and floodplain flows. Despite that, good agreement with the logarithmic-law profile is observed.

According to Schlichting (1968), the boundary layer thickness in turbulent flow, δ', is:

$$\frac{\delta'}{x} = 0.37\left(\frac{U_\infty x}{\nu}\right)^{-1/5} \quad [1]$$

where, U_∞ is the external flow stream velocity. In the case of open channel flows, U_∞ is frequently replaced by the free surface flow velocity, which, in turn, is practically equal to the maximum flow velocity of a given profile.

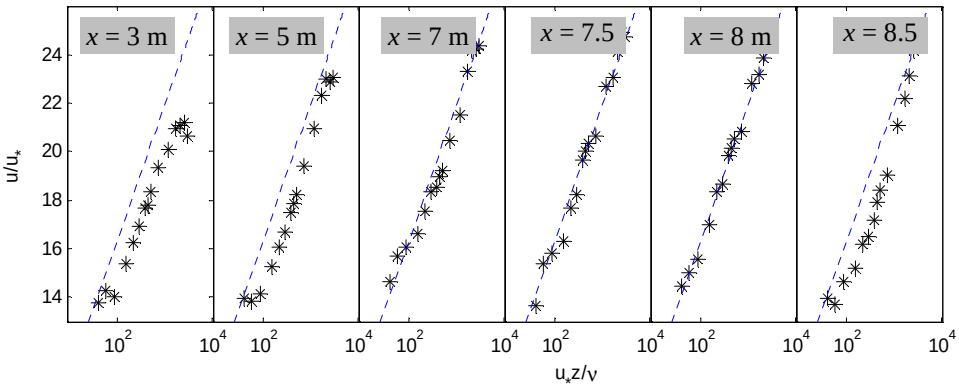

Figure 2. Vertical profiles of the streamwise velocity in the centre of the channel for flow hr030s.

The cross section x = 0 m is located at the end of the splitting plate between the main channel and the floodplain but the channel starts approximately 1 m upstream and therefore the boundary layer starts to develop at x = –1.0. Applying equation [1] to the present flow conditions, it may be concluded that, at x = 7.5 m, the boundary layer thickness should be approximately 0.145 m (ν = 1.2x10^{-6} m^{2}s^{-1} for water at 15°). Comparing the calculated boundary layer thickness with the main channel flow depth (h_{mc} = 0.1402 m), it seems reasonable to assume that the boundary layer occupies the entire flow depth at x = 7.5 m. The same is true for the remaining flow cases characterized in Table 1.

4.2 Mixing layer width

Defining U_h and U_l as the depth-averaged velocities outside of a plane mixing layer, in the regions of higher and lower velocities, respectively, the longitudinal development of the flow depends on the non-dimensional parameter U_h/U_l (*e.g.* Pope 2000).

According to Champagne *et al.* (1976), the longitudinal spreading rate parameter, S_p, can be defined as:

$$S_p = \frac{U_c}{U_s}\frac{d\delta}{dx} \qquad [2]$$

where δ is the mixing layer width, $U_s = U_h - U_l$ and $U_c = 1/2(U_h + U_l)$.

In the case of plane mixing layers, the longitudinal spreading rate parameter, S_p, must be constant according to Pope (2000). Values of S_p equal to 0.097 or ranging from 0.06 to 0.11 were observed by Champagne *et al.* (1976) and by Dimotakis (1991), respectively. The variation in the measured values of S_p from one experiment to another is partly attributed to the state of the flow leaving the splitter plate (*cf.* Slessor *et al.* 1998).

The characteristic width of the flow (*i.e.* mixing layer width), $\boldsymbol{\delta}$, can be defined using different criteria for the mixing length. For 0< α <1, the lateral position y_α can be determined by:

$$U_{y_\alpha} = U_h + \alpha U_s \qquad [3]$$

In Figure 3, the definitions of $U_{0.1}$, $U_{0.9}$, $y_{0.1}$ and $y_{0.9}$ are schematically represented for a typical depth-averaged velocity profile of a compound channel flow.

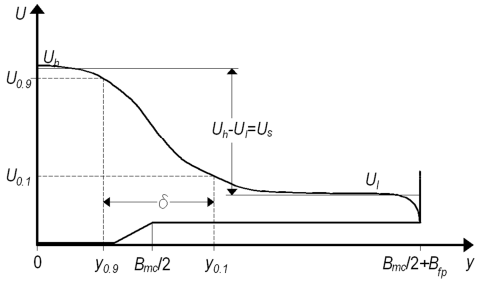

Figure 3. Definitions of the mixing layer, first criterion.

The criterion proposed by Pope (2000), defines the mixing layer width, δ, as the difference between spanwise positions $y_{0.9}$ and $y_{0.1}$:

$$\delta = \left| y_{0.9} - y_{0.1} \right| \quad [4]$$

In shallow-water flows, the bottom generates an additional source of friction that restrains the mixing layer spreading rate. Additionally, in such flows, there is a geometrical restriction to the water motion and eddies larger than the water depth cannot move or stretch in the vertical direction.

The longitudinal variation of the mixing layer width, $\boldsymbol{\delta}$, derived from the velocity fields measured in all six flows is presented in Figure 4. The growth of $\boldsymbol{\delta}$ assuming S_p = 0.06 and S_p = 0.11 (for plane mixing layers according to Dimotakis, 1991) are also included.

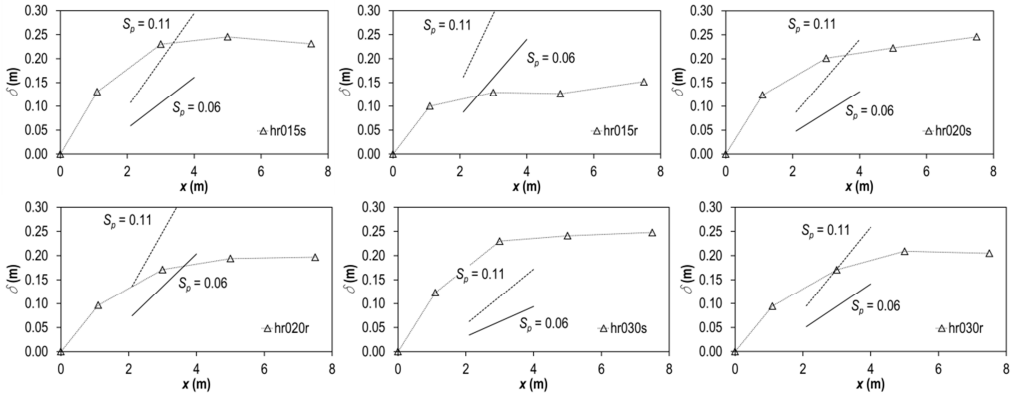

Figure 4. Longitudinal evolution of the mixing layer width.

In the upstream reach of the compound channel (x < 1.1 m), the mixing layer develops with growth rates similar to those of plane mixing layers. Higher growth rate are observed for flow cases on smooth floodplains. Due to the effect of the bottom friction, a decrease in the growth rate can be observed between the second and the third cross sections, x = 3.0 m and x = 5.0 m, respectively and further downstream. The same decrease was observed, for instance, by Uijttewaal and Booij (2000), in the development of shallow mixing layers generated by two flows with different velocities.

For flow cases with the same relative depth but different floodplain roughness it is clear that the development of the mixing layer is slower for rough floodplain and that a constant width is achieved further from the upstream section.

4.3 Longitudinal development of the streamwise velocity

The longitudinal evolution of the time-averaged streamwise velocity, $\overline{u}$, scaled by the cross section averaged streamwise velocity, U_{ave}, is shown in Figure 5. In this figure y stands for the distance to the main channel centre and z stands for the distance to the main channel bottom.

In almost all flow cases, the streamwise velocity distribution reveals some disturbances due to the entrance of the water in the channel (cross section x = 1.1 m).

The streamwise velocity distribution in the four cross sections reveals, for all flow cases, the development of the boundary layer and the mixing layer. The first may be recognized, in the region near the centre of the channel (y ≈ 0 m), by the difference in the isovels which extends until the last two cross sections, x = 5.0 m and x = 7.5 m.

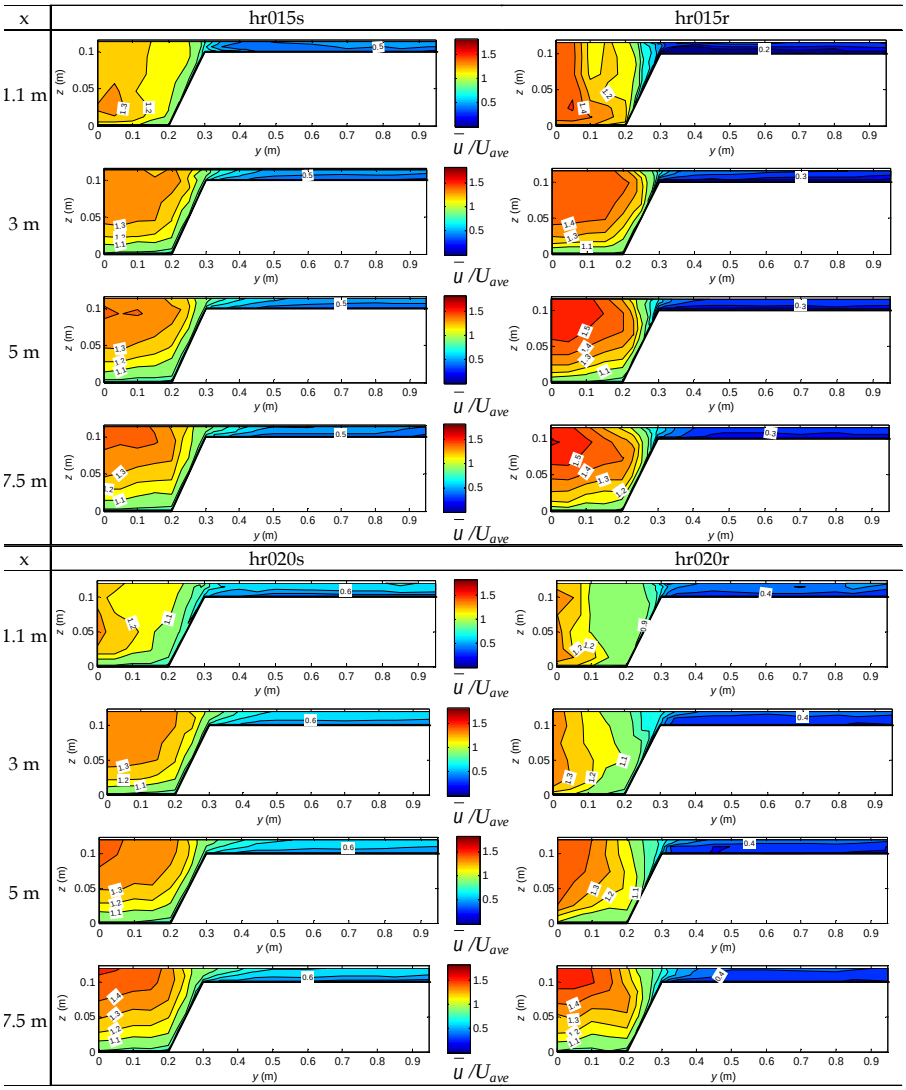

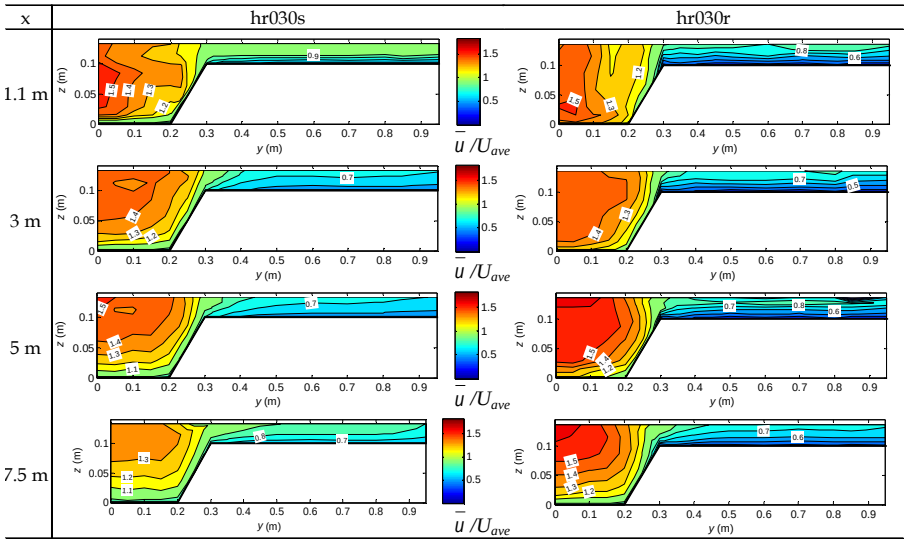

Figure 5. Cross section distribution of the streamwise velocity along the compound channel.

The development of the interaction between the flows in the main channel and in the floodplains is particularly evident in flow case hr015r. From $x = 3.0$ m to $x = 7.5$ m, the streamwise velocity in the main channel decreases due to the interaction with the slower floodplain flow. That effect leads to a deformation in the isovels, especially in the region above the bankfull level. The opposite effect is observed in the floodplain flow. Along the longitudinal direction, it is observed that the floodplain flow is accelerated due to the interaction of the main channel flow.

4.4 Longitudinal evolution of the lateral shear stress

The lateral shear stresses were also obtained from the velocity measurements. The longitudinal evolution of the lateral shear stress in the vertical plane, $-\rho\overline{u'v'}$, is presented in Figure 6.

The magnitude of the peak of the lateral shear stress increases along the longitudinal direction. It was found that the roughness in the floodplains enhances the lateral shear stress near the interface between the main channel and the floodplain.

The turbulent shear layer spreads laterally towards the main channel and floodplain as downstream distance x rises. In accordance with Booij and Tukker (2001), the large-scale horizontal eddies develop and have dimensions larger than the flow depth in the main channel.

The highest shear regions and the peaks of lateral shear stress are located close to the main channel edge. Along the longitudinal direction, these regions and peaks are downwards. This region is located in the same lateral position (approximately $y = 0.28$ m) for almost all flow cases and longitudinal cross sections. This position falls close to the location of the centre of the mixing layer, $y_{0.5}$. This small shift of the peak in relation with the edge (at $y = 0.3$ m) was also observed by Shiono and Knight (1991) for data of Series 2 in FCF-SERC, with an equivalent aspect ratio in the main channel, the same side slope of 45°, and with relative depth 0.25.

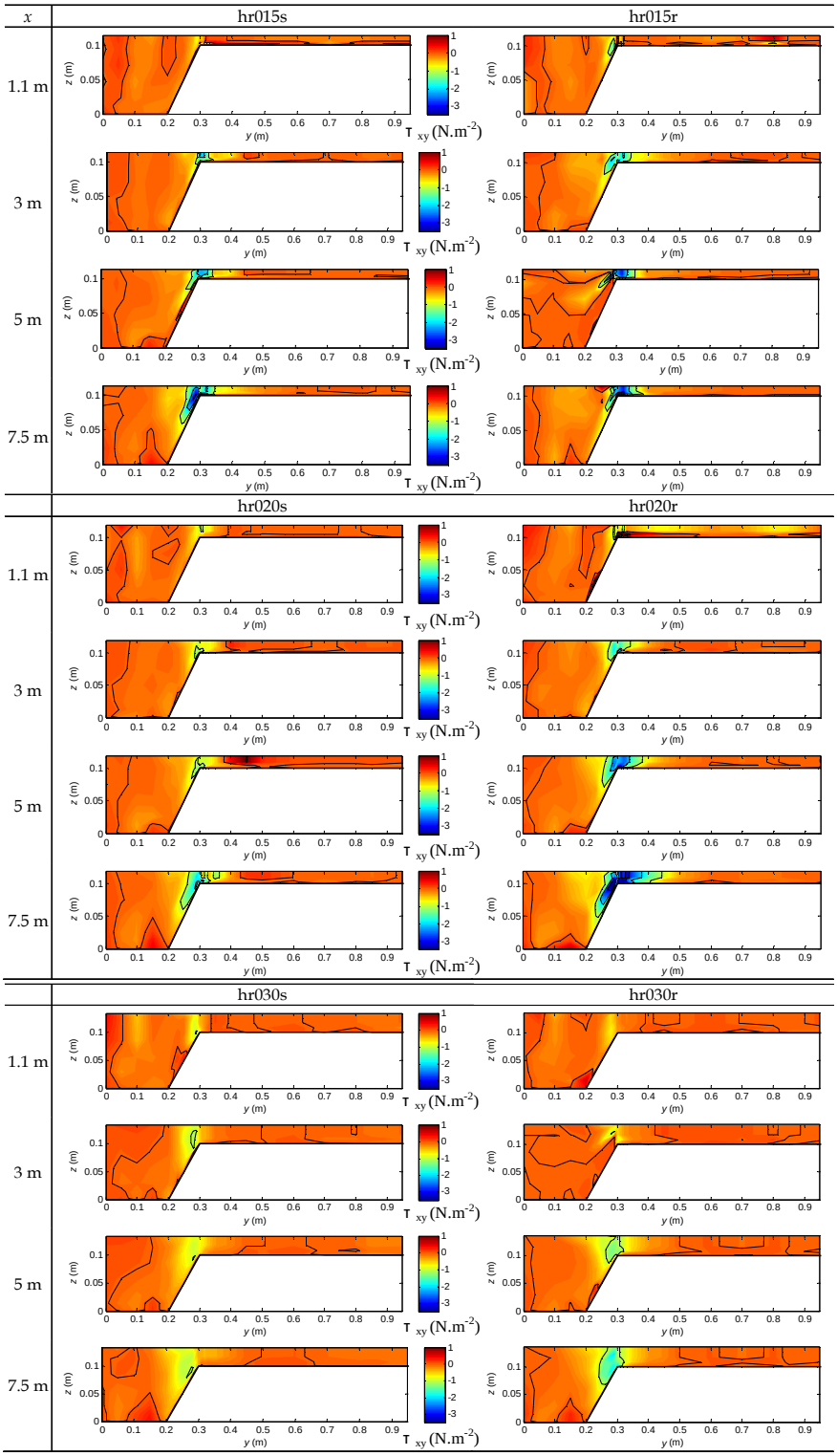

Figure 6. Cross section distribution of the lateral shear stress along the compound channel.

5. Conclusions

The development of the interaction between the flows in the main channel and in the floodplains is particularly evident in flow cases with synthetic grass covering the floodplains. Between the cross section 3.0 m and 7.5 m from the inlet section, the streamwise velocity in the main channel decreases due to the interaction with the slower floodplain flow. That effect leads to a deformation in the isovels, especially in the region above the bankfull level. Along the longitudinal direction, the floodplain flow is accelerated due to the interaction of the main channel flow.

In the upstream reach of the compound channel, the mixing layer develops with growth rates similar to those of free shear mixing layers. Due to the effect of the bottom friction, the growth rate decreases between the second and the third cross sections.

For flow cases with the same water depth and different floodplain roughness, a higher growth rate is observed for flows on smoother floodplains while a constant mixing layer width is achieved further from the inlet section.

Acknowledgments

The authors wish to acknowledge the financial support of the Portuguese Foundation for Science and Technology through the project NETFLUV (RECI/ECM-HID/0371/2012).

References

Alavian, V. and Chu, V. H. (1985) "Turbulent exchange flow in shallow compound channel", Proceedings 21th IAHR Congress, Melbourne, vol. 3, 446–451.

Booij, R. and Tukker, J. (2001) "Integral model of shallow mixing layers", Journal of Hydraulic Research, vol. 39 (2), 169–179.

Bousmar, D.; Rivière, N.; Proust, S.; Paquier, A.; Morel, R. and Zech, Y. (2005) "Upstream discharge distribution in compound-channel flumes", Journal of Hydraulic Engineering, vol. 131 (5), 408–412.

Champagne, F. H.; Pao, Y. H. and Wygnanski, I. J. (1976) "On the two-dimensional mixing region", Journal of Fluid Mechanics, vol. 74 (2), 209–250.

Chu, V. H., Wu, J. H. and Khayat, R. E. (1983) "Stability of turbulent shear flows in shallow channel", Proc. 20th Congress IAHR, Moscow, vol. 3, 128–133.

Dimotakis, P. E. (1991) "Turbulent free shear layer mixing and combustion". High-Speed Flight Propulsion Systems (ed. S. Murthy Curran and E. T.), Washington: AIAA, 265–340.

Fernandes, J.N.; Leal, J. B. and Cardoso, A. H. (2012) "Analysis of flow characteristics in a compound channel: comparison between experimental data and 1D numerical simulations" Urban Environment, Proceedings of the 10th Urban Environment Symposium, vol. 19, 249–262.

Goring, D. G. and Nikora, V. I. (2002) "Despiking acoustic Doppler velocimeter records", Journal of Hydraulic Engineering, vol. 128 (1), 117–126.

Pope, S. B. (2000) "Free shear flows". In Turbulent flows, pp. 139–144, Cambridge University.

Roy, A. G.; Biron, P. and de Serres, B. (1996) "On the necessity of applying a rotation to instantaneous velocity measurements in river flows", Earth Surface Processes and Landforms, vol. 21 (9), 817- 827.

Schlichting, H. (1968) “Boundary-layer theory”, 6th Ed., McGraw Hill Book, Co. Inc., New York, U.S.A., 748 pp.

Shiono, K. and Knight, D. W. (1991) “Turbulent open channel flows with variable depth across the channel”, Journal of Fluid Mechanics, vol. 222, 617–646.

Slessor, M. D.; Bond, C. L. and Dimotakis, P. E. (1998) “Turbulent shear-layer mixing at high Reynolds numbers: effects of inflow conditions”, Journal of Fluid Mechanics, 376, 115-138.

Uijttewaal, W. S. J. and Booij, R. (2000) "Effects of shallowness on the development of free-surface mixing layers", Physics of fluids, vol. 12 (2), 392–420.

Vermaas, D. A.; Uijttewaal, W. and Hoitink, A. J. F. (2011) “Lateral transfer of streamwise momentum caused by a roughness transition across a shallow channel”, Water Resources Research, vol. 47 (W02530).

Wygnanski, I. and Fiedler, H. E. (1970) ‘‘The two-dimensional mixing region”, Journal of Fluid Mechanics, vol. 41(2), 327–361.

Yule, A.J. (1972) “Two-dimensional self-preserving turbulent mixing layers at different free stream velocity ratios”, Aeronautical Research Council. Reports and memoranda. Department of the Mechanics of Fluids, University of Manchester.